

THE DIGGING AND HOLDING CAPACITY OF ANCHORS

Miedema, S.A.¹, Kerkvliet, J., Strijbis, D., Jonkman, B., Hatert, M. v/d²

ABSTRACT

In dredging and offshore anchors are used for positioning, but also for operations (the cutter suction dredger). In all cases it is evitable that a proper estimation of the holding capacity is very useful when designing the application. The holding capacity of anchors depends on the digging depth, the soil mechanical properties and of course the dimensions and the shape of the anchor. The digging depth also depends on the soil mechanical properties and the shape of the anchor. Now the first question is of course how is the digging depth related to the soil mechanical properties and the shape of the anchor and the second question is, how does this relate to the holding capacity. By means of deriving the equilibrium equations of motion of the anchor and applying the cutting theories, the digging behavior of anchors can be simulated. The main challenges are, how to model the shape of the anchor and how to apply the existing cutting theories to this complex shape. This paper gives a first attempt to derive equilibrium equations based on the cutting theory of Miedema (1987).

Keywords: Dredging, anchors, holding capacity, soil mechanics

INTRODUCTION

This paper is the result of assignments carried out by students for the Offshore Moorings course of the MSc program Offshore Engineering of the Delft University. In this study an analysis is made of the penetration behavior of an anchor in sand. The following points are being taken into account.

- The geometry of the anchor and how to simplify it.
- What happens when the anchor penetrates the soil?
- Which forces will occur during penetration?
- How to solve this mathematically?

First of all, the most common anchors on the market are analyzed and a general anchor geometry will be chosen. This chosen geometry will be simplified to a 2D geometry, which will be realistic for a first analysis.

After this step the penetration behavior of an anchor will be described in different phases, such a way that it is clear and easy to understand. Forces on the soil layer, fluke, shank and mooring line forces will be defined and analyzed. The forces will be described as a function of the geometries including the relevant variable angles.

THE GEOMETRY OF THE ANCHOR

While searching for the best simplified anchor geometry, knowledge of the most common anchors on the market is needed. Vrijhof anchors gives a good overview of the most common anchors. Two types of anchors can be considered, horizontal load anchors and vertical load anchors. The vertical load anchor can withstand both horizontal and vertical mooring forces. The horizontal anchor or drag embedment anchor can only resist the horizontal loads. The drag embedment anchor is mainly used for catenary moorings, where the mooring line arrives the seabed horizontally. The vertical load anchor is used in taut leg mooring systems, where the mooring line arrives at a certain angle the seabed. A good starting-point for this case is to analyze the horizontal load anchor, because this anchor is often used and will form an adequate challenge. To determine a simplified geometry of this horizontal anchor an actual figure of this anchor is needed. In the figures 1 and 2, a sketch of the selected anchor can be found.

¹ Associate Professor in Dredging Engineering & Educational Director of Offshore Engineering, Delft University of Technology, Mekelweg 2, 2628 CD Delft, The Netherlands, +31-15-2788359, s.a.miedema@3me.tudelft.nl.

² Students in Offshore Engineering, Delft University of Technology.



Figure 1. Examples of anchors.

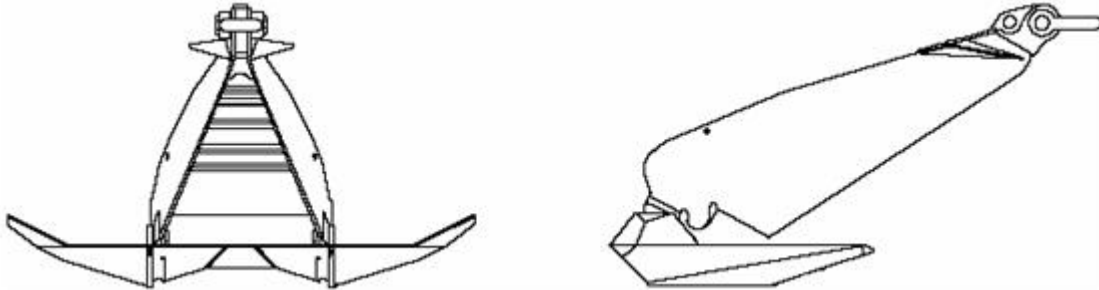


Figure 2. The geometry of anchors.

The actual blade (fluke) on the anchor that will penetrate the soil is represented by the horizontal part of the above given figure. The shank is represented by the other part of the anchor. On the end of the anchor an anchor shackle can be found. A first simplification will be made by modeling the anchor as a 2D model. Hereby all the calculations will be made easier, but the geometry is still too complex to determine all the forces. A second simplification can be made by supposing the anchor as two straight lines as can be seen in figure 3. This simplification is allowed, because this is a conceptual (first) model. When all the forces and the penetration curve of this simple model are known, a much more complicated model can be made.

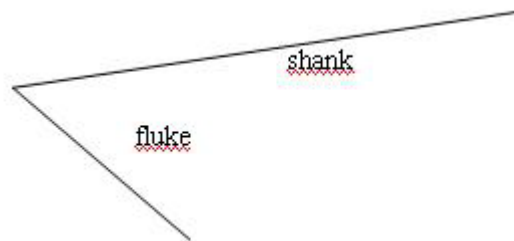


Figure 3. The definition of fluke and shank.

For the rest of the case a few assumptions must be made. First, the type of soil will be sand, this way the cohesion and adhesion effects can be neglected. As a next assumption, it is considered that the anchor penetrates the soil at a very low velocity. Therefore inertia and water tension can also be neglected. Several constraints were also made to simplify the 3D force analysis into a 2D analysis. This way several shear zones can be neglected. As a final assumption, the force acting on the point of the fluke will be neglected. This force is low considering a big anchor and will be fully cancelled by the force perpendicular on the shank.

SOIL RESISTANCE TO EMBEDDED ANCHOR LINE

The forces on the embedded anchor line can be seen as a separate system in the anchor burial process and will be treated first. Up until 1989 the work reported on embedded anchor chains was basically theoretical. Values of the design parameters such as the effective chain width in sliding (B_s), the effective chain width in bearing (B_b) and the bearing capacity factor in clay (N_c) were suggested, but little experimental proof confirmed their validity. With respect to general practice, the effective chain widths can be expressed in terms of the nominal chain diameter (D):

$$B_s = EWS * D \quad (1)$$

$$B_b = EWB * D \quad (2)$$

Where EWS and EWB are the parameters to express the effective widths in sliding and bearing, respectively.

Vivatrat et al. (1982) developed the analytical model of a chain inside soil by assuming the chain length inside soil as a summation of short line segments and expressing the equilibrium conditions of each segment. The effective width parameters EWS and EWB proposed were 10 and 2.6, respectively and the use of a value for N_c between 9 and 11 was suggested.

Yen and Tofani (1984) performed laboratory measurements on sliding and bearing soil resistances on a $\frac{3}{4}$ inch diameter stud-link chain in very soft silt. During cutting and sliding tests, the maximum soil resistances were established to be mobilized within a small movement of chain, even less than half a link. The EWS parameter can be determined from laboratory tests and varies between 5.7 and 8.9. The N_c factor at a particular depth was found to be between 7.1 and 12.1, considering the EWB parameter to be 2.37.

Using the finite segment approach, Dutta (1986, 1988) derived the nodal equilibrium equations for chain segments and proposed a simple calculation method. This study showed good agreement with the results obtained by the analytical method used by Vivatrat et al. (1982).

Degenkamp and Dutta (1989) derived a more accurate analytical model of embedded chain under soil resistance and a simple calculation procedure. They used a soil model to accurately predict the soil resistances to the chain inside soil and estimated critical design parameters, such as effective widths of chain, based on laboratory tests.

Assuming: (1) Chain elements are inextensible; (2) due to the chain shift, the soil medium suffers an undrained loading condition; (3) soil in the vicinity of the chain reaches limit state of stress and thereby develops ultimate soil resistances; and (4) the shear strength and weight of the soil over a chain element are constant. Extensive testing led to the next values:

$$\begin{array}{ll} \text{For very soft (Su = 5 kPa) clay:} & \text{EWB} = 2.5, \quad \text{EWS} = 8.0 \\ \text{For firm (Su = 34 kPa) clay:} & \text{EWB} = 2.3, \quad \text{EWS} = 7.2 \end{array}$$

Grote (1993) used the exact same approach and values obtained by Degenkamp and Dutta (1989) to determine the force distribution and geometric profile of the embedded anchor line in his work to simulate the kinematic behavior of work anchors.

Neubecker and Randolph (1994, 1995) derived closed form expressions for both the load development and chain profile to avoid the numerical solution by an incremental integration technique used by Degenkamp and Dutta (1989) and simplify the procedure. Their work corroborates the results found by Degenkamp and Dutta.

THE KINEMATIC BEHAVIOR OF DRAG ANCHORS IN CLAY

Grote (1993) derived a dynamic model to describe the anchor embedment. The forces on the anchor consist of its weight, shear and normal forces on both fluke and shank and the tension force from the anchor line pulling the anchor.

The fluke force is calculated with a transformation of the cutting formula of Miedema (1987). Grote states that the force on the fluke depends on the depth and velocity of the anchor and a constant, containing soil specific properties. The second force on the fluke, is a front force on the fluke caused by the bearing capacity of the surrounding soil. This same force is present at the shank of the anchor. They are both calculated with the formula for the bearing resistance of a strip footing formulated by Terzaghi.

Steward (1992) published methods to describe the kinematic behavior of drag anchors in cohesive soils. These methods were simplified by Neubecker and Randolph (1995) who formulated bearing capacity and moment equilibrium calculations utilizing two fundamental anchor resistance parameters. The assumption that a drag anchor travels parallel to its flukes is widely accepted. Therefore the authors expressed a geotechnical resistance force acting on the anchor parallel to the direction of the fluke.

Neubecker and Randolph (1994, 1995) also developed an expression for the anchor chain tension and angle at the anchor padeye assuming the chain angle at the seabed is zero.

Thorne (1998) developed a theory from geotechnical principals, without the use of any site or anchor specific correlations. His predictions of the anchor movement showed good agreement with nine full scale tests covering three different sites and five anchor types. The equations used are based on the proposition that no movement will occur until the soil forces acting parallel to the fluke are overcome. The motion of the anchor results in the soil around the shank failing in bearing capacity on the underside and in shearing on the base and sides, exerting on the shank the maximum force of which the soil is capable. This is also true for other elements which have to be dragged through the soil like shackles, palms and stabilizers.

THE KINEMATIC BEHAVIOR OF DRAG ANCHORS IN SAND

Le Lievre and Tabatabaee (1981) proposed a limit equilibrium method. This method has been shown to give reasonable predictions of the ultimate holding capacity of drag anchors in sand, for a given depth of embedment. However, several assumptions in the analytical procedure make it unsuitable for application to a drag anchor during embedment, and hence the approach does not allow prediction of the depth to which the anchor will embed, and thus the actual capacity.

Grote (1993) defined a force model with the same problem approach for clay as for sand grounds only the formula's for the ground resistances are different.

Neubecker and Randolph (1995) based their approach on the method of LeLievre and Tabatabaee (1981). They extended this method to incorporate:

- a more realistic 3-dimensional failure pattern in the soil,
- a force acting on the back of the fluke.

The latter modification is particularly important at shallow penetrations, when the bearing capacity of the anchor shank is insufficient to provide equilibrium. The authors suggested that the force on the shank is dependent on its size and shape and should be calculated from a bearing capacity viewpoint.

Dickin (1988) presented an overview of some of the various methods that have been developed to evaluate the pullout resistance of a flat plate. It was considered that the simple method of Majer (1955) consistently underestimated the pullout capacity of the flat plate, while the model of Vermeer and Sutjiadi (1985) gave predictions that compared well with observations. Neubecker and Randolph incorporated the model of Vermeer and Sutjiadi into the drag anchor problem.

PENETRATION PHASES

Phase 1

No penetration

In this first situation the anchor lies on the bed of soil and the fluke/shank angle will be considered as a minimum. When pulling on the mooring line the anchor will scratch over the seabed, see Figure 4. A bed of soil will be formed in front of the fluke and will give some resistance. Because of this resistance, an angle κ will reach its maximum at a certain point. At that certain point, the bed of soil in front of the fluke will give his highest resistance and it will become easier to penetrate than scratching over the seabed. When the assumption of a perfect sharp fluke point is made, the point load can be neglected.

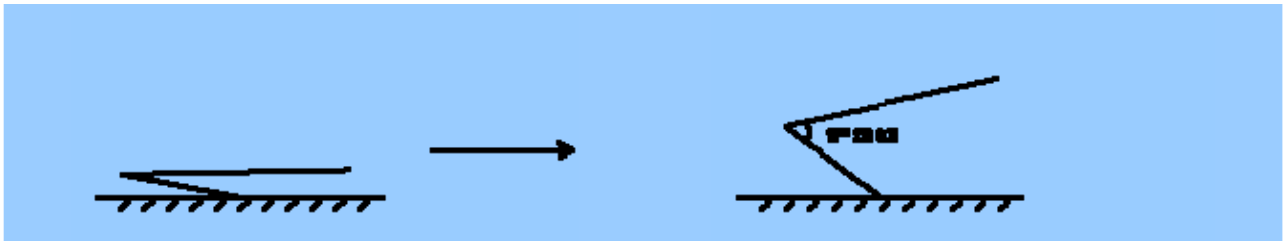


Figure 4. The anchor on top of the soil in phase 1.

Phase 2

Penetration causes fluke forces.

When the fluke starts to penetrate (Figures 5 and 6), the cutting theory of Miedema (1987), can be used. Forces that will play a role in the force balance are the fluke forces. When the angles on the fluke are considered, a few assumptions can be made. First of all the fluke/shank angle κ will be constant and will have its maximum value. The internal friction and the external friction angles are also constant. These parameters are only depending on the material of the anchor and soil mechanical properties.

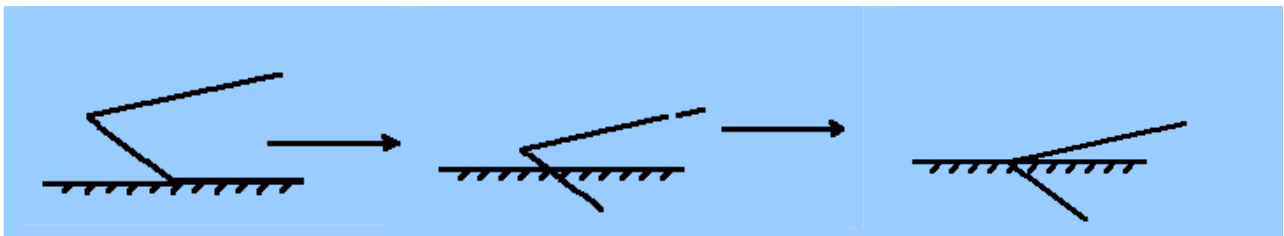


Figure 5. The fluke penetrating the soil in phase 2.

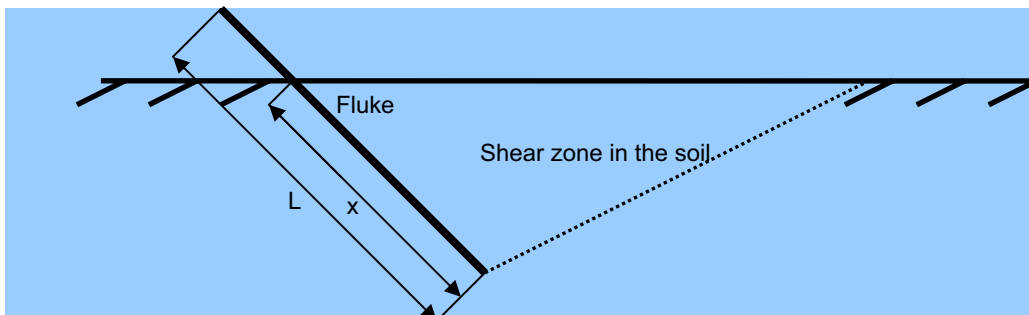


Figure 6. The fluke in the soil.

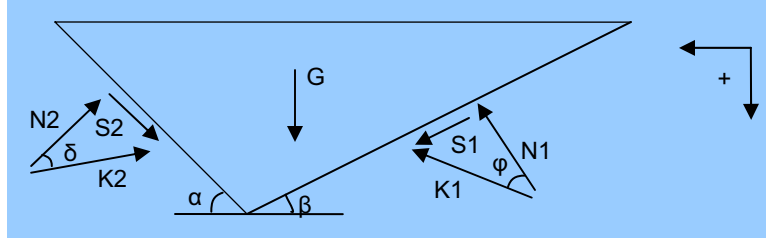


Figure 7. The forces on the soil layer.

As discussed before the cohesion, adhesion, inertial forces and water tension can be neglected. According to Figures 7 and 8, a force balance can be calculated.

The shear force and the normal force are related according:

$$S_1 = N_1 \tan \varphi \quad (3)$$

$$S_2 = N_2 \tan \delta \quad (4)$$

The grain forces will be:

$$K_1 = \sqrt{(S_1^2 + N_1^2)} \quad (5)$$

$$K_2 = \sqrt{(S_2^2 + N_2^2)} \quad (6)$$

The weight of the soil can be given as a force according:

$$G = \left(\frac{x^2 \sin^2 \alpha}{2 \tan \alpha} + \frac{x^2 \sin^2 \alpha}{2 \tan \beta} \right) \cdot \gamma \quad (7)$$

Horizontal equilibrium of forces:

$$K_1 \cdot \sin(\beta + \varphi) - K_2 \cdot \sin(\alpha + \delta) = 0 \quad (8)$$

Vertical equilibrium of forces:

$$-K_1 \cdot \cos(\beta + \varphi) + G - K_2 \cdot \cos(\alpha + \delta) = 0 \quad (9)$$

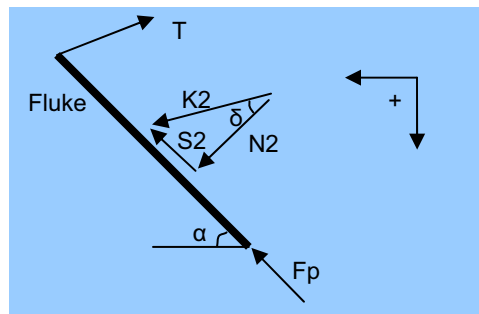


Figure 8. The forces on the fluke.

The force K_2 on the fluke is important to determine the horizontal and vertical acting forces on the fluke (Figure 8).

$$K_2 = \frac{G \cdot \sin(\beta + \varphi)}{\sin(\alpha + \beta + \varphi + \delta)} \quad (10)$$

The following forces are acting on the fluke blade:

- The Horizontal Force

$$F_h = K_2 \cdot \sin(\alpha + \delta) \quad (11)$$

- The Vertical Force

$$F_v = K_2 \cdot \cos(\alpha + \delta) \quad (12)$$

The force F_p can be neglected as discussed before.

Phase 3

Penetration causes fluke and shank forces.

In this situation the fluke is completely covered by sand and the shank will become an extra factor which will cause penetration resistance, see Figures 9 and 10. For the shank the cutting theory of Miedema (1987), can't be used. The strip footing theory, as described in Verruijt (2000), will be used for determining the shank resistance. The maximum shank resistance acts when the complete shank is penetrated.



Figure 9. The shank penetrating the soil in phase 3.

In this paragraph you will find the modeling of the forces on the fluke and the shank. The influences of the angles will be given. The cutting theory of Miedema (1987) is still valid for the fluke part of the anchor forces. For determining the forces on the shank, the strip footing theory, as described in Verruijt (2000), will be used. For phase 3, two shear zones are taken into account. This will lead to a geometry as shown in figure 11.

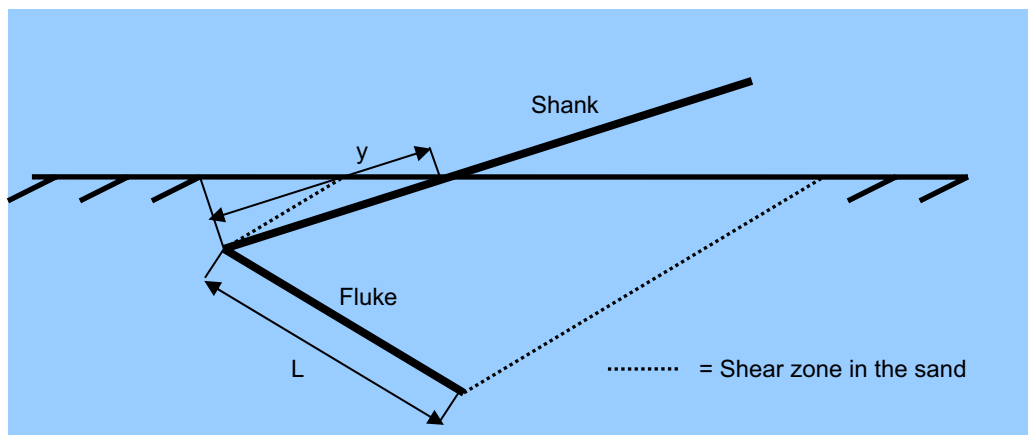


Figure 10. The fluke and shank in the soil.

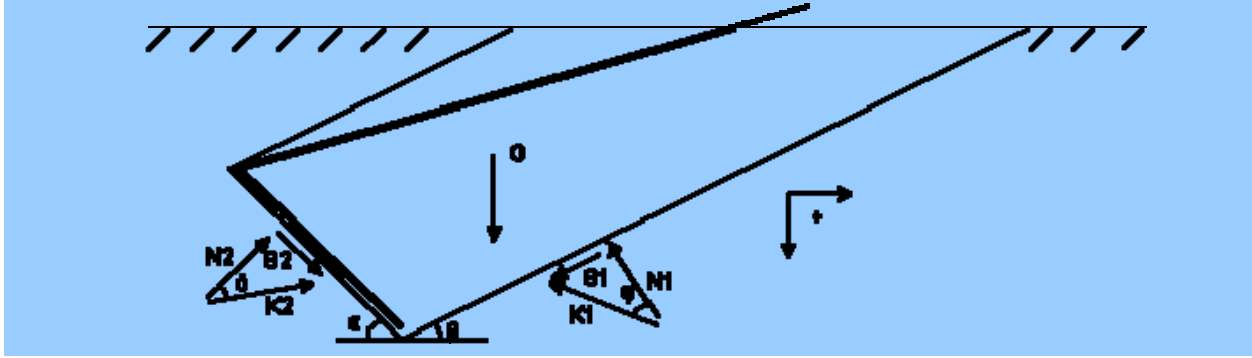


Figure 11. Forces on the soil layer.

As discussed before; the cohesion, adhesion, inertial forces and water tension can be neglected. For the Figures 11 and 12, a force balance can be calculated. The shear force and the normal force are related according:

The shear force and the normal force are related according:

$$S_1 = N_1 \tan \varphi \quad (13)$$

$$S_2 = N_2 \tan \delta \quad (14)$$

The grain forces will be:

$$K_1 = \sqrt{(S_1^2 + N_1^2)} \quad (15)$$

$$K_2 = \sqrt{(S_2^2 + N_2^2)} \quad (16)$$

The weight of the soil can be determined by using the geometry of Figure 12, so the weight of the soil will be:

$$G = A_{\text{soil}} \cdot \gamma \quad (17)$$

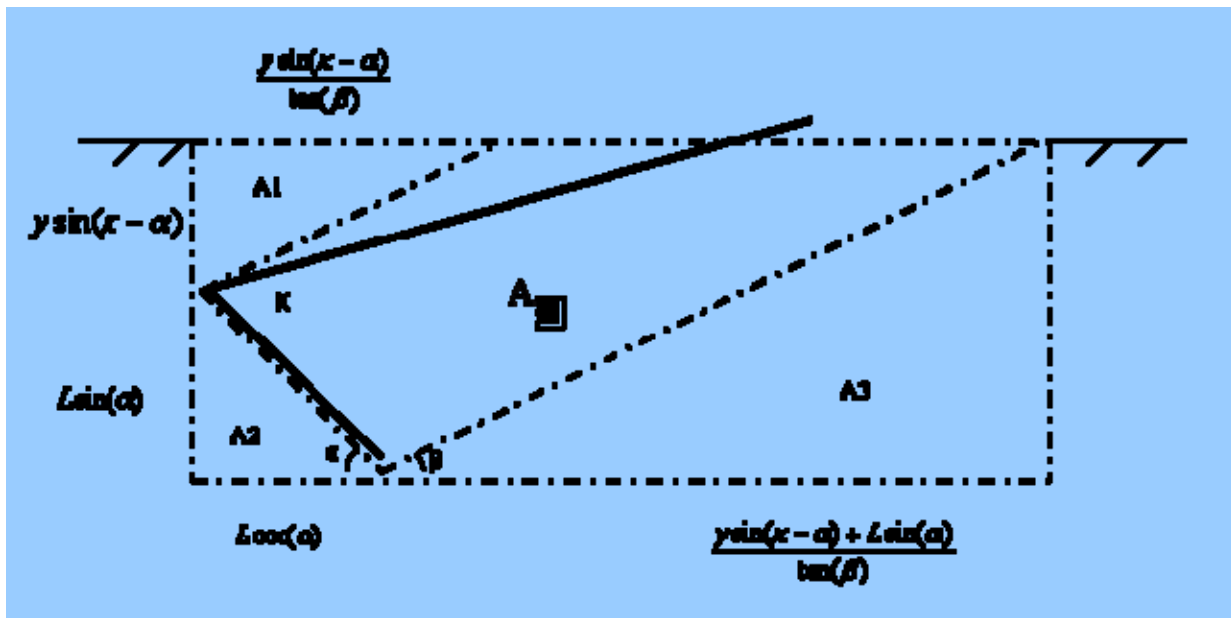


Figure 12. The dimensions of the soil layer.

with:

$$A_{\square} := (y \cdot \sin(\kappa - \alpha) + L \cdot \sin(\alpha)) \cdot \left(L \cdot \cos(\alpha) + \frac{y \cdot \sin(\kappa - \alpha) + L \cdot \sin(\alpha)}{\tan(\beta)} \right) - \left(\frac{y^2 \cdot \sin(\kappa - \alpha)^2}{2 \cdot \tan(\beta)} \right) - \frac{1}{2} \cdot L^2 \cdot \sin(\alpha) \cdot \cos(\alpha) - \left(\frac{(y \cdot \sin(\kappa - \alpha) + L \cdot \sin(\alpha))^2}{2 \cdot \tan(\beta)} \right) \quad (18)$$

Forces on the fluke and the shank

For the determination of the forces on the fluke and the shank, Figure 13, two different theories will be used. For the fluke the cutting theory of Miedema is valid, therefore forces on the soil layer and on the fluke are the same as discussed in phase 2. For the forces on the shank the strip footing theory can be used. This theory is based on the fundamentals of Brinch Hansen and is a generalization of the Prantl theory. This can be found in Verruijt (2000).

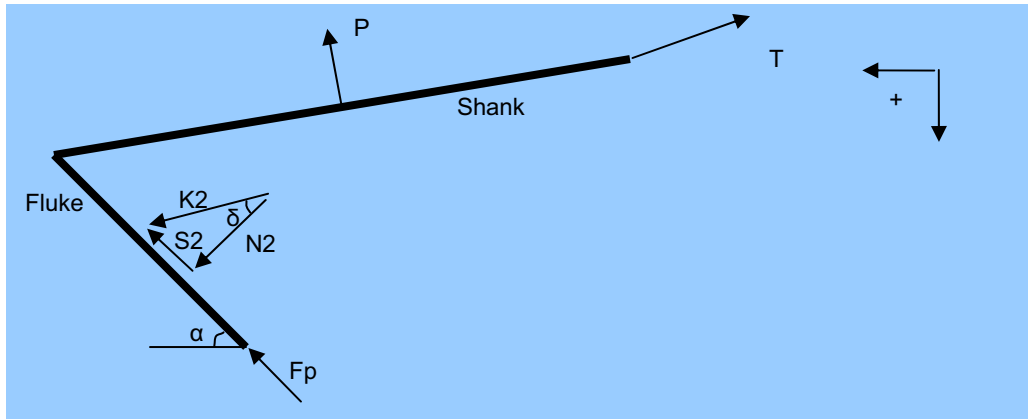


Figure 13. The forces on the anchor.

To determine the friction Brinch Hansen force P on the shank we can make use of:

$$P = i_c s_c c N_c + i_q s_q q N_q + i_\gamma s_\gamma \frac{1}{2} \gamma B N_\gamma \quad (19)$$

where c is cohesion and q is the external load on the soil

Because c and q are zero in this case (no cohesion and no external force on the soil), P will only be a function of the soil weight part of the function, so:

$$P = i_\gamma s_\gamma \frac{1}{2} \gamma B N_\gamma \quad (20)$$

Hereby i_γ is a correction factor for inclination factors of the load. The factor s_γ is a shape factor for the shape of the load.

In this case only a load perpendicular to the soil will be considered, so i_γ will be removed from the formula.

Inserting N_γ :

$$P = \left(1 - 0,3 \frac{B}{y}\right) B^2 y \gamma \left(\frac{1 + \sin \phi}{1 - \sin \phi} e^{\pi \tan \phi} - 1\right) \tan \phi \quad (21)$$

Now the friction part of the shank has to be determined. For the friction of the shank, the next formula is valid:

$$F_{\text{friction}} = \sigma_n \tan(\delta) y h \quad (22)$$

It is possible now to plot the results for P and F_{friction} (see Figure 14) then it is possible to find out if the downward force of the fluke is big enough to pull the shank through the seabed and further.

It is also possible now to make a total force and moment balance, to predict the trajectory of the anchor.

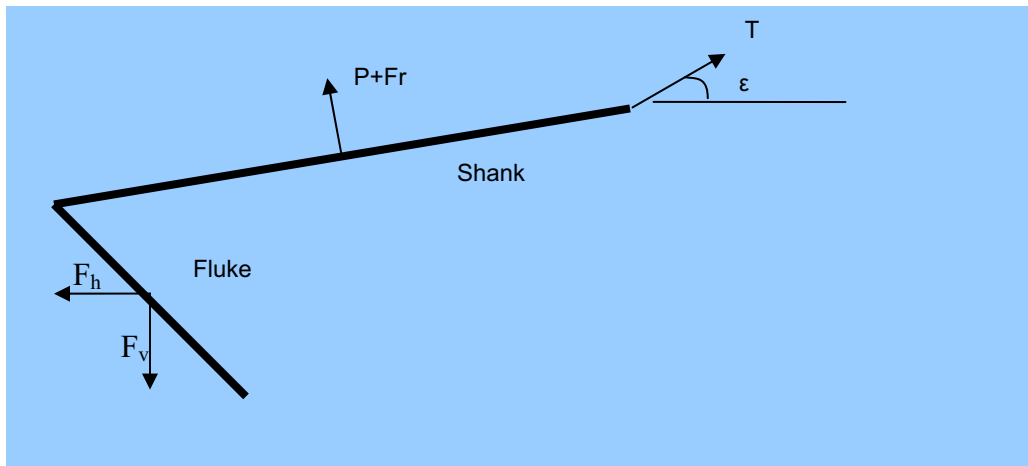


Figure 14. The forces on the anchor.

Phase 4

Penetration causes fluke forces, shank forces and mooring line forces.

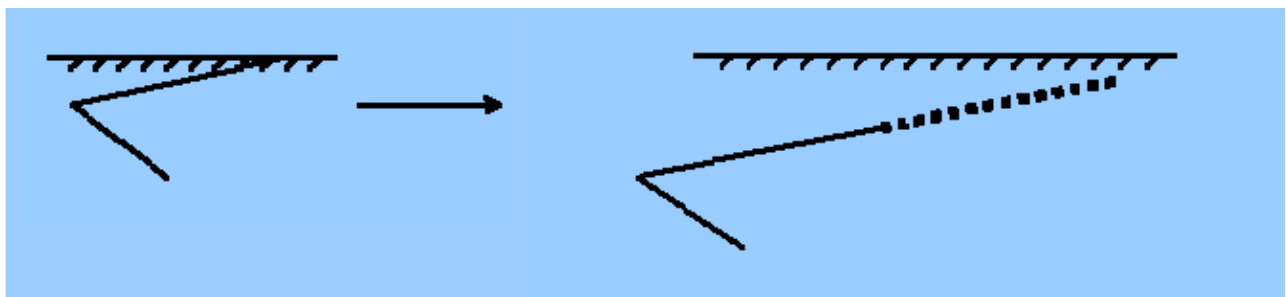


Figure 15. The mooring line penetrating the soil in phase 4.

The fluke and the shank are completely covered by sand (Figures 15 and 16). When there is still no equilibrium, a part of the mooring line will enter the soil. The mooring line penetration will lead to an extra factor which will cause penetration resistance. The anchor becomes stable when there is a balance between the vertical and horizontal forces on the anchor part, which is covered by sand.

In this phase you will find the modeling of the forces on the fluke, the shank and the mooring line. The cutting theory of Miedema is still valid for the fluke part of the anchor forces. For determining the forces on the shank and the mooring line we will use the strip footing theory as discussed in Verruijt.

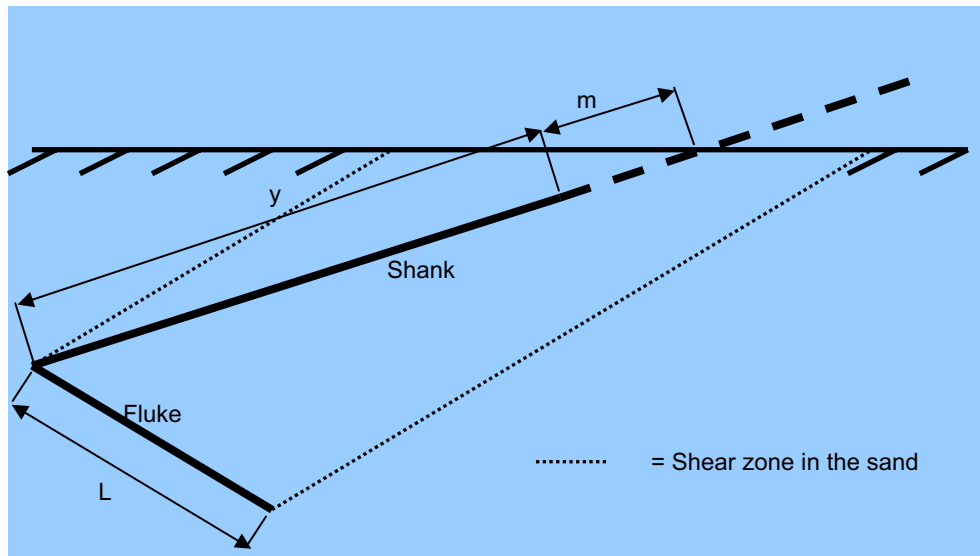


Figure 16. Fluke, shank and mooring line in the soil.

The soil layer properties can be interpreted in a same way as described in phase 3. So this way the function for G is still valid.

To determine the forces on the anchor for this situation the theory as discussed in phase 3 is valid. For the mooring line forces (Figures 17 and 18) we will also use the Brinch Hansen theory as discussed in Verruijt (2000).

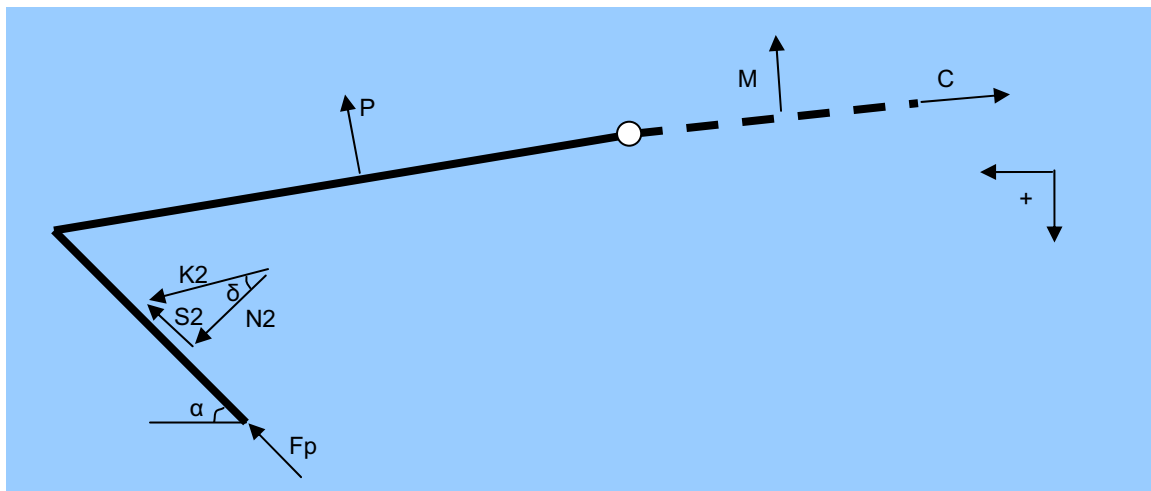


Figure 17. Forces on the fluke, shank and mooring line.

The penetration of the mooring line causes resistance perpendicular to this line (penetration resistance, see Figure 19). This effect is noticeable in all soil conditions. The type of mooring line will determine the value of this resistance. Think of a wire rope mooring line which penetrates deeper (less resistance) than a chain mooring line. During the penetration process of the anchor, the resistance increases when depth increases, which is related to the position of the anchor.

The mooring line penetration can be described by the following geometry. When looking at the point where the anchor becomes stable, a force and moment balance can be made out of all the forces on the anchor and mooring line. In fact this is the moment where the anchor reaches his maximum holding capacity.

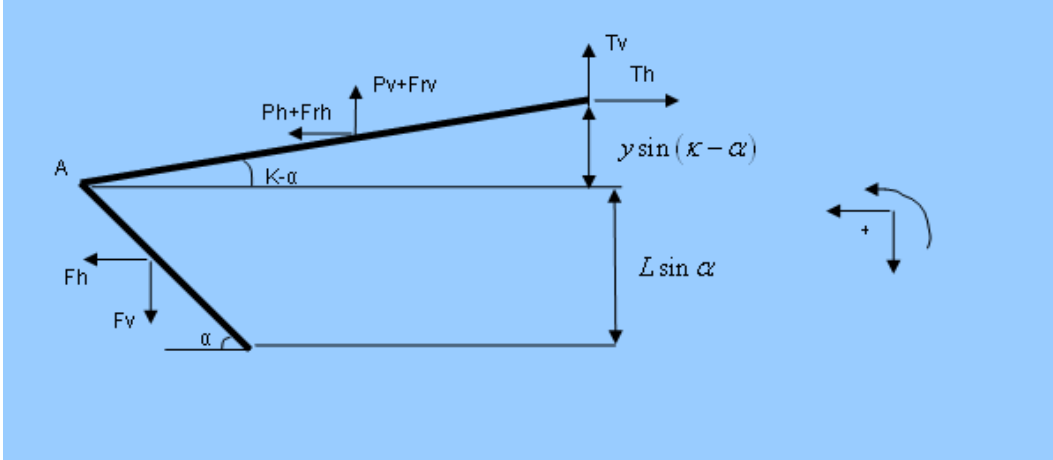


Figure 18. The forces on the anchor.

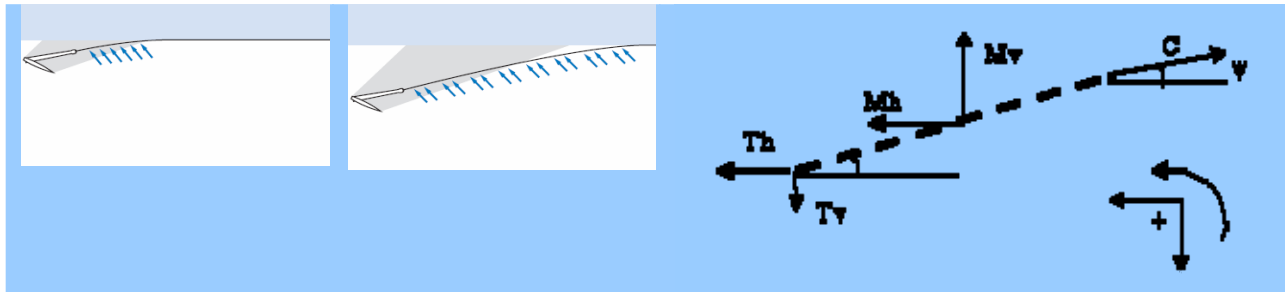


Figure 19. The forces on the mooring line.

Vertical equilibrium of forces:

$$F_v - P_v - F_{rv} - M_v - T_v = 0 \quad (23)$$

Horizontal equilibrium of forces:

$$F_h + P_h + F_{rh} + M_h - T_h = 0 \quad (24)$$

Moment balance to point A:

$$-F_v \cdot \frac{1}{2} L \cos \alpha - F_h \cdot \frac{1}{2} L \sin \alpha + (P_v + F_{rv}) \cdot \frac{1}{2} y \cos(\kappa - \alpha) + (P_h + F_{rh}) \cdot \frac{1}{2} y \sin(\kappa - \alpha) + T_v \cdot y \cos(\kappa - \alpha) + T_h \cdot y \sin(\kappa - \alpha) = 0 \quad (25)$$

CONCLUSIONS AND RECOMMENDATIONS

In the penetration behavior the different forces and moments in all four phases can be described with the theory dealt with, in this document. These forces and moments are a function of the anchor geometry. The holding capacity of the anchor is described as well as a function of the depth and the geometry. To predict the trajectory of the anchor during the penetration, one has to find a relationship between the different forces and moments on the anchor and the trajectory of the anchor. The anchor trajectory will stop when the different forces are in equilibrium, or when the pull force will be too high for that particular anchor, at a certain depth. In the last case, the pull force necessary to penetrate deeper in the soil is higher than the maximum holding capacity of that particular anchor at a certain depth to that point the maximum holding capacity is reached (see Figure 20). When pulling further, the anchor will be pulled out and loses his function.

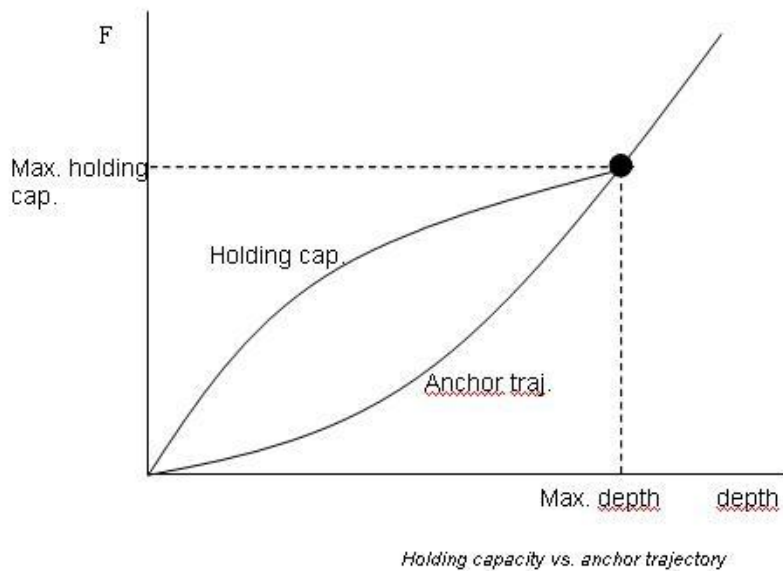


Figure 20. Holding capacity vs. anchor trajectory.

LIST OF SYMBOLS USED

α	Angle of the fluke in the sand	rad
β	Angle of the shear zone	rad
φ	Internal friction angle of the sand	rad
δ	External friction angle fluke/sand	rad
χ	Length of the fluke in the sand	m
γ	Density of the in situ sand	ton/m ³
κ	Angle between fluke and shank	rad
L	Total fluke length	m
y	Length of the shank in the sand	m
B	Width of the shank	m
σ_n	Normal stress on the area of the shank	N/m ²
h	Height of the shank	m
M	Resistance on mooring line	kN/m
C	Catenary force	kN
T	Anchor pull force	kN

REFERENCES

- Degenkamp, G. and Dutta, A. (1989). "Behaviour of Embedded Mooring Chains in Clay During Chain Tensioning." Offshore Technology Conference, Paper 6031.
- Degenkamp, G. and Dutta, A. (1989). "Soil Resistances to Embedded Anchor Chain in Soft Clay." *Journal of Geotechnical Engineering*, Vol 115, No. 10
- Det Norske Veritas. (2002). "Design and Installation of Plate Anchors in Clay." Recommended Practice DNV-RP-302.
- Dunnavant, T.W. and Kwan, C-T.T. (1993). "Centrifuge Modeling and Parametric Analysis of Drag Anchor Behavior." Offshore Technology Conference, Paper OTC 7202.
- Grote, B.J.H. (1993). "Simulation of Kinematic Behavior of Workanchors." Faculty of Mechanical Engineering, Offshore Engineering Major, Report nr: 92.3.GV.3034, 93.3.GV.4074 and 93.3.GV.4167, Delft University of Technology.
- House, A. (1998). "Drag Anchor and Chain Performance in Stratified Soils." Geomechanics Group, Report 1319, The University of Western Australia.
- Lammes, R.R. and Siemers, R.W. (1988). "Soil Mechanics of Drag Embedment Anchor in Sand." Faculty of Civil Engineering, Offshore Engineering Major, Delft University of Technology.
- Lin, K. and Randolph, M.F. (1998). "Numerical Analysis of Stresses and Displacements in Layered Soil Systems." Geomechanics Group, Report G1334, The University of Western Australia.
- Miedema, S.A., "Calculation of the Cutting Forces when Cutting Water Saturated Sand". Ph.D. Thesis, Delft University of Technology, September 15th 1987.
- Mierlo, R. v. (2005). "Anchor Trajectory Modeling." Faculty of Mechanical Engineering, Offshore Engineering Major, Delft University of Technology.
- Murff, J.D., Randolph, M.F. & Elkhatab, S., Kolk, H.J., Ruinen, R.M., Strom, P.J. and Thorne, C.P. (2005). "Vertically Loaded Plate Anchors for Deepwater Applications." *Frontiers in Offshore Geotechnics ISFOG*.
- Ruinen, R.M. (2005). "Influence of Anchor Geometry and Soil Properties on Numerical Modeling of Drag Anchor Behavior in Soft Clay." *Frontiers in Offshore Geotechnics ISFOG*.
- Neubecker, S.R. and Randolph, M.F. (1996). "The Static Equilibrium of Drag Anchors in Sand." *Canadian Geotechnical Journal*, 33: 574-583
- Neubecker, S.R. and Randolph, M.F. (1996). "The Kinematic Behavior of Drag Anchors in Sand." *Canadian Geotechnical Journal*, 33: 584-594
- Neubecker, S.R. and Randolph, M.F. (1995). "Performance of Embedded Anchor Chains and Consequences for Anchor Design." Offshore Technology Conference, Paper OTC 7712.
- Neubecker, S.R. and Randolph, M.F. (1995). "Profile and Frictional Capacity of Embedded Anchor Chains." *Journal of Geotechnical Engineering* Vol. 121, No. 11
- Neubecker, S.R. and Randolph, M.F. (1995). "The Performance of Drag Anchor and Chain Systems in Cohesive Soil." Geomechanics Group, Report G1168, The University of Western Australia.
- Neubecker, S.R. and Randolph, M.F. (1994). "Profile and Frictional Capacity of Embedded Anchor Chains." Geomechanics Group, Report G1142, The University of Western Australia.
- O'Neill, M.P. and Randolph, M.F. (1998). "The Behaviour of Drag Anchors in Layered Calcareous Soils." Geomechanics Group, Report G1329, The University of Western Australia.
- O'Neill, M.P., Randolph, M.F. and House, A.R. (1998). "The Behaviour of Drag Anchors in Layered Soils." Geomechanics Group, Report G1346, The University of Western Australia.
- Stewart, W.P. (1992). "Drag Embedment Anchor Performance Prediction in Soft Soils." Offshore Technology Conference, Paper OTC 6970.
- Thorne, C.P. (1998). "Penetration and Load Capacity of Marine Drag Anchors in Soft Clay."
- Verruijt, A., "Soil Mechanics". Lecture Notes, Delft University of Technology, 2000.